Occurrence Frequency of CO Outflows in Massive Protostellar Candidates

Kee-Tae Kim[1,2] and S. E. Kurtz[3]

ABSTRACT

We mapped 12 massive protostellar candidates in the CO J=2−1 line, which in combination with Zhang et al. (2005) completes an unbiased survey of outflows for all 48 sources with l>50° in a sample of 101 massive protostellar candidates. We detected outflows in 10 sources, implying 88% occurrence frequency of outflows for the 48 sources. This supports the conclusion of previous studies that bipolar outflows are an integral component in the formation process of massive stars. The vast majority of the observed outflows are much more massive (>10 $M_\odot$) and energetic (>100 $M_\odot$ km s^{-1}) than outflows from low-mass protostars. They also have large mass outflow rates (>2×10^{-4} $M_\odot$ yr^{-1}), suggesting large (∼1×10^{-4} $M_\odot$ yr^{-1}) accretion rates sufficient to overcome radiation pressure of the central massive protostars. We compared the frequency distribution of collimation factors of 40 massive outflows including those of this study with that of 36 low-mass outflows from the literature, and found *no* significant difference between the two. All these results are consistent with the suggestion that massive stars form through accretion as do low-mass stars but with much higher accretion rates.

Subject headings: ISM: clouds — ISM: jets and outflows – ISM: kinematics and dynamics — stars: formation

1. Introduction

It has been well established that low-mass stars form by gravitational collapse of dense molecular cores and that accretion disks and bipolar outflows are basic building blocks of the process (Shu et al. 1987). Compared to low-mass star formation, very little is known about the formation process of massive (>8 M$_\odot$) stars, such that it is still much debated whether massive stars form in a qualitatively similar manner to low-mass stars. This debate is mainly because the radiation pressure of massive stars is strong enough to reverse materials infalling at the typical mass accretion rates

[1]Department of Astronomy, University of Illinois, 1002 West Green Street, Urbana, IL 61801

[2]Korea Astronomy & Space Science Institute, 61-1 Hwaam-Dong, Yuseong-Gu, Daejeon 305-348, Korea; ktkim@kasi.re.kr

[3]Centro de Radioastronomía y Astrofísica, UNAM, Apartado Postal 3-72, Morelia 58089, Michoacán, México; s.kurtz@astrosmo.unam.mx

observed in low-mass young stellar objects (YSOs) (Wolfire & Cassinelli 1987). There are currently two major theoretical models in competition: accretion via disks (e.g., Yorke & Sonnhalter 2002; McKee & Tan 2003) and coalescence of low-mass (proto)stars (e.g., Bonnell et al. 1998). The most convincing way to differentiate between the two models may be to investigate whether well-defined accretion disks exist around massive YSOs. But it is difficult to detect the accretion disks, if any, because they would be small (at most several hundred AU), short-lived, and easily confused by envelopes. In this study we attempt to distinguish between the two models by observing bipolar molecular outflows that are much easier to detect.

Bipolar outflows from low-mass YSOs have been extensively studied since the early 1980's (see Bachiller 1996, and references therein), while systematic studies of outflows associated with massive star formation began much later. These studies are roughly divided into two groups. The first group are single-point CO line surveys towards samples of massive YSOs in search of high-velocity molecular gas (e.g, Shepherd & Churchwell 1996a; Sridharan et al. 2002). They showed that high-velocity gas is a common feature in massive YSOs. Shepherd & Churchwell (1996a) made a CO J=1−0 line survey towards 122 massive YSOs, the vast majority of which are ultracompact (UC) HII regions, and detected high-velocity gas in 90% of the 94 sources suitable for line wing analysis. Sridharan et al. (2002) obtained a similar detection rate (84%) from a CO J=2−1 line survey of 69 massive protostellar candidates. The second group are CO line mappings of subsets of the sources that exhibit high-velocity wings (e.g., Shepherd & Churchwell 1996b; Beuther et al. 2002a). These studies investigated whether the high-velocity wings are caused by bipolar outflows and derived the physical and dynamical parameters of the outflows. Shepherd & Churchwell (1996b) mapped 10 sources with high-velocity gas and identified outflows in 5 sources. If we assume a similar detection rate for the remainder of their sample, the occurrence frequency of outflows would be about 45% for their sample. Beuther et al. (2002a) found outflows in 21 of 26 sources showing high-velocity wings in the sample of Sridharan et al. (2002), indicating a significantly higher occurrence rate (∼70%). These studies also show that bipolar outflows from massive YSOs are much more massive and energetic than those observed in low-mass YSOs (see also Ridge & Moore 2001). There is some controversy as to whether massive outflows are much less collimated than low-mass outflows (see § 3.1).

The present paper presents CO J=2−1 line maps of 12 massive star-forming regions at 27″ angular resolution (Table 1). Combining the results of this study with those of Zhang et al. (2001, 2005), we complete a census of molecular outflows for all sources with $l \geq 50°$ in a flux-limited sample of massive protostellar candidates (see § 2.1), and estimate the occurrence frequency of molecular outflows for the sample. We also examine the morphological, physical, and dynamical properties of bipolar outflows observed, and compare them with those of outflows from low-mass YSOs. The selection criteria of the sources and the details of the observations are described in § 2. The results are presented in § 3. The implications of our results for massive star formation are discussed in § 4. We summarize the main results in § 5.

2. Observations

2.1. Source Selection

Our sources are a subset of the catalog of 101 massive protostellar candidates (Molinari et al. 1996), which were selected from a complete flux-limited sample of bright IRAS point sources with far-infrared (FIR) colors similar to compact molecular cores, based on the detection of NH_3 line emission. The original sample consists of 260 IRAS point sources that satisfy flux, color, and practical criteria (Palla et al. 1991): 1) $F_{60}\geq100$ Jy and no upper limits for F_{25}, F_{60}, and F_{100}, (2) $0.61\leq\log(F_{60}/F_{25})\leq1.74$, and $0.087\leq\log(F_{100}/F_{60})\leq0.52$, (3) no positional coincidence with known HII regions, and (4) $|b|\leq10°$ and $\delta\geq-30°$. Molinari et al. (1996) surveyed NH_3 (1,1) and (2,2) lines towards 163 of the 260 sources, and detected 101 sources. Among the 101 sources, 63 ("high" group) have colors characteristic of UC HII regions, $\log(F_{25}/F_{12})\geq0.57$ and $\log(F_{25}/F_{12})\geq1.30$ (Wood & Churchwell 1989), while the remaining 38 ("low" group) have colors of $\log(F_{25}/F_{12})<0.57$. Most (∼90%) of the 101 sources have bolometric luminosities $>10^3\ L_\odot$, so they are very likely to be massive protostars that have not yet formed UC HII regions, probably because of active accretion (Molinari et al. 1996, 1998). Zhang et al. (2001, 2005) mapped 69 of the 101 sources in the CO J=2−1 line: 67 sources observed by Molinari et al. (1998) in radio continuum and 2 other sources (IRAS 00117+6412 and IRAS 06056+2131). They detected outflows in about 90% (35/39) of their sources in the Galactic longitude range $l\geq50°$. For sources at $0°<l<50°$, they could not compile reliable statistics because outflow signatures are frequently confused with other cloud components along the same lines of sight. In this study we observed 12 sources (Table 1). They include all 11 sources with $l\geq50°$ among the 34 sources not observed by Molinari et al. (1998), and IRAS 05274+3345. Thus our sample has 3 common sources (IRAS 00117+6412, IRAS 05274+3345, and IRAS 06056+2131) with the sample of Zhang et al. (2001, 2005).

2.2. CO J=2−1 Line Observations

We mapped the 12 sources in the CO J=2−1 line using the 12 m telescope[1] at Kitt Peak in 2003 January and February. The telescope has a FWHM of 27″ at 230 GHz. A 256-channel filterbank with 128 MHz bandwidth was used in parallel mode to observe both circular polarizations simultaneously, and the velocity resolution is 0.68 km s^{-1}. The system temperature varied in the range 500−700 K during the observing sessions. All the sources were mapped with 8″ spacing in position switching mode using the on-the-fly observing technique. The reference positions were checked to be free from appreciable (>0.1 K) CO emission. They were usually ∼30′ away from the sources. The pointing and focus were checked every four hours with Venus, Saturn, or DR21. The typical *rms* noise level is 0.2 K. The observed temperature ($T_{\rm R}^*$) was converted to main-beam

[1]The 12m telescope is a facility of the National Science Foundation currently operated by the University of Arizona Steward Observatory under a loan agreement with the National Radio Astronomy Observatory.

brightness temperature ($T_{\rm b}$) using the corrected main-beam efficiency ($\eta^{*}_{\rm mb}$=0.51) provided by the observatory.

3. Results

3.1. CO Maps

We detected high-velocity CO gas towards all sources in our sample with the possible exception of IRAS 06105+1756 (Table 1). Here we compared the observed full width at zero intensity (FWZI) of each CO line with that expected from the FWHM by Gaussian fit, and define a high-velocity excess if the former is greater than the latter. With the exception of one source (IRAS 22272+6358A) we find, as do Shepherd & Churchwell (1996a) in the CO J=1−0 line data, that the FWZI of the CO J=2−1 line is always >15 km s^{-1} for the sources showing high-velocity excess. The FWZI of IRAS 22272+6358A is about 12 km s^{-1} in our 0.2 K *rms* data; possibly it would be broader at the 0.02 K *rms* level of Shepherd & Churchwell (1996a).

Based on contour maps of blue- and red-shifted high-velocity gas and position-velocity diagrams, we conclude that 10 of the 11 sources host outflows; the exception is IRAS 06061+2151 (Fig. 1). In IRAS 22272+6358A only blue-shifted high-velocity gas is detected. This is consistent with the result of CO J=1−0 line observations made by Sugitani et al. (1989) at 17″ resolution. The IRAS sources are located reasonably close to the outflow centers in most cases, but they are offset from the centers by greater than the 27″ telescope beamwidth in three sources (IRAS 06103+1523, IRAS 06382+0939, IRAS 23545+6508). In these cases the IRAS sources are unlikely to be the driving sources of the outflows. Some maser sources and/or (sub)millimeter continuum sources, which are good indicators of massive star-forming sites in early evolutionary stages, are found around the outflow centers in IRAS 06382+0939 (Wolf-Chase et al. 2003) and IRAS 23545+6508 (Beuther et al. 2002b; see also Anglada & Rodríguez 2002).

The morphologies of blue- and red-lobes are roughly symmetric in five sources (IRAS 00117+6412, IRAS 05274+3345, IRAS 06056+2131, IRAS 20227+4154, IRAS 22267+6244), whereas they are asymmetric in the remaining 4 sources (IRAS 05553+1631, IRAS 06103+1523, IRAS 06382+0939, IRAS 23545+6508). Such an asymmetry is often seen in the CO maps of outflows both from low-mass and high-mass YSOs (e.g., Bontemps et al. 1996; Beuther et al. 2002a; Zhang et al. 2005). Possible explanations of this feature are the asymmetric ejection of outflow-driving agents from the central stars, the nonuniform distribution of the ambient molecular gas, and the presence of multiple outflows. There seem to be two (or more) outflows in IRAS 06056+2131. This may be true for IRAS 05274+3345 as well (see also Hunter et al. 1995). This multiplicity complicates the high-velocity gas distributions of the two regions. We estimate the physical and dynamical parameters of the two (A and B) outflows in IRAS 06056+2131 separately (see § 3.2), while we do not for the two of IRAS 05274+3345, because they are entangled in position as well as in velocity.

As noted earlier, there is some debate about the collimation of outflows from massive YSOs. Richer et al. (2000) and Ridge & Moore (2001) argued that outflows from massive YSOs are significantly less collimated than those observed in low-mass YSOs (see also Wu et al. 2004 and § 4), while Beuther et al. (2002a) suggested, based on higher-resolution (11″) CO maps, that they are better collimated than previously thought. We determine the collimation factors (f_c), defined as the ratio of outflow length to width, of the 11 observed outflows (Table 2). The values range between 1.0 and 3.8. They are greater than 2.0 for 6 sources; for comparison, Ridge & Moore (2001) reported collimation factors of $\sim$1−2. Our average collimation factor is 2.3, similar to the 2.1 value determined by Beuther et al. (2002a) for 15 outflows from massive protostellar candidates despite our factor of $\sim$2.5 lower angular resolution. This may be because all outflows in our sample are located closer to the Sun and in less crowded ($75° < l < 205°$) regions of the Galactic plane than the majority of their sources. The average value is also very similar to that (2.2) measured for 36 low-mass outflows as discussed in § 4. From our sample, IRAS 05274+3345 A, IRAS 05553+1631, and IRAS 06382+0939 are particularly well collimated with factors >3.0. In comparison, none of outflows observed by Beuther et al. (2002a) have collimation factors greater than 3.0.

3.2. Outflow Parameters

We derive the physical and dynamical parameters of the outflows in a similar way to Cabrit & Bertout (1992) and Beuther et al. (2002a). Here we assume (1) the excitation temperature of CO gas is 30 K (Molinari et al. 1996), (2) the integrated intensity ratio of CO to ^{13}CO is 10 in the line-wing velocity range (Choi et al. 1993), (3) [CO]/[H_2]=1×10^{-4} and [CO]/[^{13}CO]=89, and (4) the mean molecular weight is 2.3. We do not correct for the inclination of the outflow. Table 2 displays the results: masses M_b (blue-shifted), M_r (red-shifted), M_{out} (total), momentum P, kinetic energy E, dynamical age t, mass outflow rate $\dot{M}_{out}$, mechanical force F_m, mechanical luminosity L_m, and collimation factor f_c. The vast majority of outflows have sizes of 0.3−1.4 pc, dynamical ages of $(1-10)\times10^4$ yr, masses >10 $M_\odot$, momenta >100 $M_\odot$ km s^{-1}, and mass outflow rates of $(1-10)\times10^{-4}$ $M_\odot$ yr^{-1}. Thus these outflows are much more massive and energetic than outflows from low-mass protostars (Class 0 and Class I objects) with similar dynamical ages (e.g., Cabrit & Bertout 1992; Bontemps et al. 1996; Wu et al. 2004). This is consistent with the results of previous single-dish studies of massive YSO outflows (Shepherd & Churchwell 1996b; Beuther et al. 2002a; Zhang et al. 2005). The large estimated outflow rates suggest mass accretion rates large enough to overcome the strong radiation of the central massive stars (see § 4 for details).

3.3. Occurrence Frequency of Outflows

Zhang et al. (2001, 2005) mapped 69 of the 101 sources of Molinari et al. (1996) in the CO J=2−1 line at about 30″ grid spacing using the Kitt Peak 12 m and the Caltech Submillimeter Observatory 10 m. They detected outflows in 39 of the 65 sources that have data suitable for

outflow identification, for a detection rate of 60%. But it was practically impossible to compile reliable statistics for 26 sources in the Galactic longitude range $0^\circ < l < 50^\circ$ because of multiple cloud components in the same lines of sight. They found a much higher 90% (35/39) detection rate for 39 sources with $l \geq 50^\circ$. In this study we observed 12 sources selected from the same catalog. They are all located at $l \geq 50^\circ$. We detected in 10 sources outflows that have similar physical and dynamical properties to other outflows from massive YSOs. This indicates the outflow detection rate is 88% for all 48 sources with $l \geq 50^\circ$ in the Molinari catalog, taking into account that the two samples have 3 sources in common. It may be reasonable to expect a similar occurrence frequency of outflows for the sources at $0^\circ < l < 50^\circ$, because both groups were selected by the same criteria. The FWZI of the CO line is $\sim$10 km s^{-1} for the sources that show no distinct high-velocity wings. Assuming that the typical outflow velocity is $\sim$25 km s^{-1}, outflows at inclinations $\gtrsim 80^\circ$ would not be detected. Statistically, the fraction of those outflows is $\sim$10%. Thus this result strongly suggests that nearly all sources in the Molinari catalog have molecular outflows.

There have been several attempts to measure the occurrence frequency of molecular outflows in low-mass protostellar objects (e.g., Terebey et al. 1989; Parker et al. 1991; Bontemps et al. 1996). The detection rates range between $\sim$70% and 90%. For example, Bontemps et al. (1996) mapped 45 low-mass protostars (36 Class I and 9 Class 0 objects) of nearby (<450 pc) molecular clouds in the CO J=2−1 line, and found outflows in 75%−80% of the sources. The detection rate was higher (80%−90%) for 34 YSOs with dust continuum emission. These values are similar to the detection rate determined by this study for the Molinari sources. Therefore, bipolar outflows appear to be an integral stage in the formation process of massive stars as well, as suggested by some previous studies (e.g., Zhang et al. 2001, 2005; Beuther et al. 2002a; Wu et al. 2004).

4. Implications for Massive Star Formation

As mentioned earlier, the formation process of massive stars is still poorly understood. Two major theoretical models are currently competing: accretion and coalescence. If massive stars form by accretion as do low-mass stars, all massive protostars would generate massive and powerful outflows. Probably this is not true for the coalescence model where massive stars form from the collision of low-mass (proto)stars. There are three major collision units, such as stars, disks(/outflows), and cores, and six types of collisions are possible among the three (Bally & Zinnecker 2005). Only if disk-disk collisions dominate the other types of collisions, and if the collisions do not profoundly disrupt the outflows of low-mass (proto)stars, might one expect that most massive protostars have massive and energetic outflows. Thus the observed high occurrence frequency of outflows can not be easily explained by the coalescence model. On the other hand, the collimation degree of outflows could be very different between the two models. The masses of massive outflows are usually one order of magnitude larger than those (<1 $M_\odot$) of low-mass outflows. If massive stars form by coalescence, this suggests that a massive outflow may arise after multiple collisions. In that case, although the outflows of low-mass protostars survive the collisions, the resulting massive outflow

might be highly impulsive and poorly collimated like the OMC-1 outflow observed by Allen & Burton (1993). In contrast, one would expect relatively well-collimated outflows around massive protostars in the accretion model.

Most outflows observed by this study do *not* seem to be very different from many low-mass outflows in collimation (e.g., Bontemps et al. 1996). In order to investigate this quantitatively, we compare the frequency distribution of collimation factors of 40 massive outflows with that of 36 low-mass outflows. In this comparison we use the values derived by Lada (1985), Beuther et al. (2002a), and this study for 14, 15, and 11 massive outflows, respectively. The associated IRAS sources almost always have bolometric luminosities from 10^3 to 10^5 $L_\odot$, and the majority of them are massive protostellar candidates. For low-mass outflows we adopt the values determined by Lada (1985) for 12 sources, and estimate collimation factors for 24 sources using the CO maps provided by Myers et al. (1988), Schwartz et al. (1988), Parker et al. (1991), and Bontemps et al. (1996), which are systematic single-dish studies of multiple sources mainly at relatively low ($30''-45''$) resolutions. Here we exclude CO maps that do not cover the full outflows. Most of their driving sources are Class 0 and Class I objects. Figure 2 shows the result. Though a higher fraction of low-mass outflows have collimation factors $\geq$3.5, the two distributions appear to be quite similar and the average values, 2.2, are the same. This does not agree with the finding of Wu et al. (2004) for a sample of 231 YSOs that the average collimation factors are 2.8$\pm$2.2 and 2.1$\pm$1.0 for low-mass and massive outflows, respectively. This discrepancy may be mostly because of different resolutions of the data used for low-mass outflows in the analyses, even if we cannot exclude the possibility that some intrinsic difference exists between low-mass and massive outflow collimations. Our analysis includes only single-dish data for all low-mass outflows, while the Wu's analysis contains significantly higher-resolution single-dish and interferometer data for many low-mass outflows, which can reveal highly-collimated outflows. There are 10 outflows with collimation factors >5 in the Wu sample of low-mass outflows. Unless they are included, the average collimation factor is close to 2.2. On the other hand, it is not straightforward to identify highly-collimated outflows around massive YSOs even in interferometer data, because massive stars tend to form in groups and clusters where multiple outflows may overlap. For example, Beuther et al. (2002c) found at least 3 outflows, two of which are highly collimated, in the interferometer data of the massive star-forming region 05358+3543. The three could not be separated in single-dish data and the collimation factor of the combined outflow was measured to be 2.0 (Beuther et al. 2002a).

It is widely accepted that low-mass outflows are momentum-driven by highly-collimated jets and/or wide-angle winds from the central (proto)stars (Königl & Pudritz 2000; Shu et al. 2000). If massive outflows are produced by the same mechanisms, the mass accretion rates can be estimated from the observed outflow rates under the assumption of momentum conservation between jets/winds and outflows. The ratio of wind mass-loss rate to accretion rate is typically ~0.1 in the highly-collimated jet model (Königl & Pudritz 2000) and ~0.3 in the wide-angle wind model (Shu et al. 2000). Assuming that the velocity ratio of winds to outflows is around 20 (see § 4.2 of Beuther et al. 2002a), the mass accretion rate would be 20%−50% of the outflow rate. The average value of

the observed outflow rates is 5×10^{-4} $M_\odot$ yr^{-1} (Table 2), so the accretion rate is $\sim1\times10^{-4}$ $M_\odot$ yr^{-1}. This value is much greater than the typical accretion rates of (10^{-7}–10^{-5}) $M_\odot$ yr^{-1} expected and measured in low-mass YSOs (e.g., Shu 1977; Bontemps et al. 1996). It is also large enough to overcome the radiation pressure of the central stars, which have bolometric luminosities $\leq2\times10^4$ $L_\odot$ (Walmsley 1995). Therefore, the results of this study appear to support the accretion model rather than the coalescence model.

5. Conclusions

We mapped 12 massive protostellar candidates in the CO J=2−1 line, which in combination with Zhang et al. (2005) completed a census of bipolar molecular outflows for all 48 sources with l>50° in the Molinari catalog of 101 massive protostellar candidates. We detected outflows in 10 of the 12 sources, indicating 88% occurrence frequency of outflows in the 48 sources. The observed outflows are much more massive (>10 $M_\odot$) and energetic (>100 $M_\odot$ km s^{-1}) than those observed in low-mass YSOs. These results imply that almost all sources of the Molinari catalog have very massive and powerful molecular outflows. Thus bipolar outflows appear to be a ubiquitous phenomenon in massive star formation as in low-mass star formation, as suggested by some previous studies.

Nearly all outflows observed by this study have mass outflow rates $>2\times10^{-4}$ $M_\odot$ yr^{-1}, suggesting large accretion rates of $\sim1\times10^{-4}$ $M_\odot$ yr^{-1}. These values are much greater than the typical accretion rates expected and measured in low-mass YSOs and are large enough to overcome the radiation pressure of the central massive protostars. We compared the collimation factors of 40 massive outflows with those of 36 low-mass outflows, and found *no* significant difference between them. This can be naturally understood in the accretion model, but cannot be easily explained by the coalescence model. Therefore, it is likely that accretion plays a dominant role in the formation process of massive stars, although we cannot exclude the possibility that coalescence plays a role in some special circumstances.

We acknowledge support from the Laboratory for Astronomical Imaging at the University of Illinois and NSF AST 0228953.

REFERENCES

Allen, D. A., & Burton, M. G. 1993, Nature, 363, 54

Anglada, G., & Rodríguez, L. F. 2002, RMxA&A, 38, 13

Bachiller, R. 1996, ARA&A, 34, 111

Bally, J., & Zinnecker, H. 2005, AJ, 129, 2281

Beuther, H., Schilke, P., Gueth, F., McCaughrean, M., Andersen, M., Sridharan, T. K., & Menten, K. M. 2002c, A&A, 387, 931

Beuther, H., Schilke, P., Menten, K. M., Motte, F., Sridharan, T. K., & Wyrowski, F. 2002b, ApJ, 566, 945

Beuther, H., Schilke, P., Sridharan, T. K., Menten, K. M., Walmsley, C. M., & Wyrowski, F. 2002a, A&A, 383, 892

Bonnell, I. A., Bate, M. R., & Zinnecker, H. 1998, MNRAS, 298, 93

Bontemps, S., Andre, P., Terebey, S., & Cabrit, S. 1996, A&A, 311, 858

Brand, J. et al. 1994, A&AS, 103, 541

Cabrit, S., & Bertout, C. 1992, A&A, 261, 274

Carpenter, J. M., Snell, R. L., & Schloerb, F. P. 1995, ApJ, 450, 201

Choi, M., Evans, N. J. II, & Jaffe, D. T. 1993, ApJ, 417, 624

Dame, T. M., & Thaddeus, P. 1985, ApJ, 297, 751

Hunter, T. R., Testi, L., Taylor, G. B., Tofani, G., Felli, M., & Phillips, T. G. 1995, A&A, 302, 249

Königl, A. & Pudritz, R. E. 2000, in Protostars and Planets IV, ed. V. Mannings, A. P. Boss, & S. S. Russell (Tucson: Univ. Arizona Press), 759

Lada, C. J. 1985, ARA&A, 23, 267

McKee, C. F., & Tan, J. C. 2003, ApJ, 585, 850

Molinari, S., Brand, J., Cesaroni, R., & Palla, F. 1996, A&A, 308, 573

Molinari, S., Brand, J., Cesaroni, R., Palla, F., & Palumbo, G. G. C. 1998, A&A, 336, 339

Myers, P. C., Heyer, M., Snell, R. L., & Goldsmith, P. F. 1988, ApJ, 324, 907

Palla, F., Brand, J., Comoretto, G., Felli, M., & Cesaroni, R. 1991, A&A, 246, 249

Parker, N. D., Padman, R., & Scott, P. F. 1991, MNRAS, 252, 442

Ridge, N. A., & Moore, T. J. T. 2001, MNRAS, 378, 495

Schwartz, P. R., Gee, G., & Huang, Y.-L. 1988, ApJ, 327, 350

Shepherd, D. S., & Churchwell, E. 1996a, ApJ, 457, 267

Shepherd, D. S., & Churchwell, E. 1996b, ApJ, 472, 225

Shu, F. H. 1977, ApJ, 214, 488

Shu, F. H., Adams, F. C., & Lizano, S. 1987, ARA&A, 25, 23

Shu, F. H., Najita, J. R., Shang, H., & Li, Z.-Y. 2000, in Protostars and Planets IV, ed. V. Mannings, A. P. Boss, & S. S. Russell (Tucson: Univ. Arizona Press), 789

Sridharan, T. K., Beuther, H., Schilke, P., Menten, K. M., & Wyrowski, F. 2002, ApJ, 566, 931

Sugitani, K., Fukui, Y., Mizuni, A., & Ohashi, N. 1989, ApJ, 342, L87

Szymczak, M., Hrynek, G., & Kus, A. J. 2000, A&AS, 143, 269

Terebey, S., Vogel, S. N., & Myers, P. C. 1989, ApJ, 340, 472

Walmsley, M. 1995, RMxAC, 1, 137

Wolf-Chase, G., Moriarty-Schieven, G., Fich, M., & Barsony, M. 2003, MNRAS, 344, 809

Wolfire, M. G., & Cassinelli, J. P. 1987, ApJ, 319, 850

Wood, D. O. S., & Churchwell, E. 1989, ApJ, 340, 265

Wouterloot, J. G. A., Brand, J., & Fiegle, K. 1993, A&AS, 98, 589

Wu, Y., Wei, Y., Zhao, M., Shi, Y., Yu, W., Qin, S., & Huang, M. 2004, A&A, 426, 503

Yorke, H. W., & Sonnhalter, C. 2002, ApJ, 569, 846

Zhang, Q., Hunter, T. R., Brand, J., Sridharan, T. K., Molinari, S., Kramer, M. A., & Cesaroni, R. 2001, ApJ, 552, L167

Zhang, Q., Hunter, T. R., Brand, J., Sridharan, T. K., Cesaroni, R., Molinari, S., Wang, J., & Kramer, M. A. 2005, ApJ, 625, 864

Table 1. Source Summary

Source[a] Number	IRAS Name	Type[a]	α(J2000) ($^{h\ m\ s}$)	δ(J2000) ($^{\circ}\ '\ ''$)	l ($^{\circ}$)	b ($^{\circ}$)	d (kpc)	$L_{\rm bol}$ ($L_{\odot}$)	Maser H_2O[b]	Maser CH_3OH[c]	CO J=2−1 Wings	CO J=2−1 Outflow
2	00117+6412	H	00 14 27.7	+64 28 46	118.961	+1.893	1.8	1.38E3	Y	N	Y	Y
10	05274+3345	H	05 30 45.6	+33 47 52	174.197	−0.078	1.6	4.35E3	Y	Y	Y	Y
14	05553+1631	H	05 58 13.9	+16 32 00	192.161	−3.815	2.0[d]	5.20E3	Y	N	Y	Y
15	06056+2131	H	06 08 41.0	+21 31 01	189.032	+0.784	2.0[d]	1.04E4	Y	Y	Y	Y
16	06061+2151	H	06 09 07.8	+21 50 39	188.796	+1.033	2.0[d]	1.11E4	Y	Y	Y	N
19	06103+1523	H	06 13 15.1	+15 22 36	194.934	−1.227	4.6	1.91E4	N	N	Y	Y
21	06105+1756	H	06 13 28.3	+17 55 30	192.723	+0.040	3.4	1.60E4	N	N	N?	N
27	06382+0939	H	06 41 02.7	+09 36 10	203.205	+2.080	0.8	1.63E2	N	N	Y	Y
124	20227+4154	L	20 24 31.4	+42 04 17	79.885	+2.552	1.7[e]	2.64E3	Y	N	Y	Y
146	22267+6244	H	22 28 29.4	+62 59 44	107.504	+4.488	0.5	1.10E2	N	N	Y	Y
147	22272+6358A	H	22 28 52.3	+64 13 43	108.186	+5.519	1.2	1.97E3	N	Y	Y	Y
163	23545+6508	H	23 57 05.2	+65 25 11	117.315	+3.142	1.3	3.89E3	N	N	Y	Y

[a]Source number and High/Low (H/L) designation of Molinari et al. (1996).

[b]Wouterloot et al. (2004) and Brand et al. (1994).

[c]Szymczak et al. (2000).

[d]Assumed to be located in the Gemini OB1 cloud complex (Carpenter et al. 1995), in which case the $L_{\rm bol}$'s were re-calculated with new distances from the values given by Molinari et al. (1996).

[e]Assumed to be associated with the Cygnus X complex (Dame & Thaddeus 1985).

Table 2. Outflow Properties Derived from CO J=2−1 Line Data

IRAS Name	Size (pc)	$M_{\rm b}$ ($M_\odot$)	$M_{\rm r}$ ($M_\odot$)	$M_{\rm out}$ ($M_\odot$)	P ($M_\odot$ km s^{-1})	E (10^{46}) (10^{46} erg)	t (10^4) (10^4 yr)	$\dot{M}_{\rm out}$ (10^{-4}) ($M_\odot$ yr^{-1})	$F_{\rm m}$ (10^{-3}) ($M_\odot$ km s^{-1} yr^{-1})	$L_{\rm m}$ ($L_\odot$)	$f_{\rm c}$
00117+6412	0.7	6.6	5.6	12.1	213	3.7	3.8	3.2	5.6	7.8	1.0
05274+3345A/B[a]	1.4	20.1	14.7	34.8	481	6.7	9.9	3.5	4.9	5.4	3.3/1.6
05553+1631	1.7	29.0	8.9	37.9	609	9.9	11.1	3.4	5.5	7.1	3.4
06056+2131A	1.4	21.7	29.4	51.1	694	9.4	10.1	5.1	6.9	7.4	2.0
06056+2131B	1.0	35.5	7.7	43.2	617	8.9	7.5	5.8	8.3	9.5	1.0
06103+1523	2.2	28.0	37.1	65.1	995	15.4	14.4	4.5	6.9	8.5	2.7
06382+0939	0.9	4.3	8.9	13.2	193	2.9	5.8	2.3	3.3	4.0	3.8
20227+4154	1.2	56.0	34.7	90.6	2937	98.3	3.8	23.8	77.3	205.1	2.1
22267+6244	0.3	2.0	1.8	3.8	66	1.2	1.6	2.4	4.2	5.9	1.5
22272+6358A[b]	0.4	1.4	0.0	1.4	16	0.2	3.4	0.4	0.5	0.4	···
23545+6508	0.8	3.5	2.1	5.5	61	0.7	7.2	0.8	0.9	0.7	2.8

[a]The properties of 05274+3345A and 05274+3345B are not separately estimated except for the collimation factor, because the two are entangled both in position and velocity.

[b]Only blue-shifted high-velocity gas is detected (see the text).

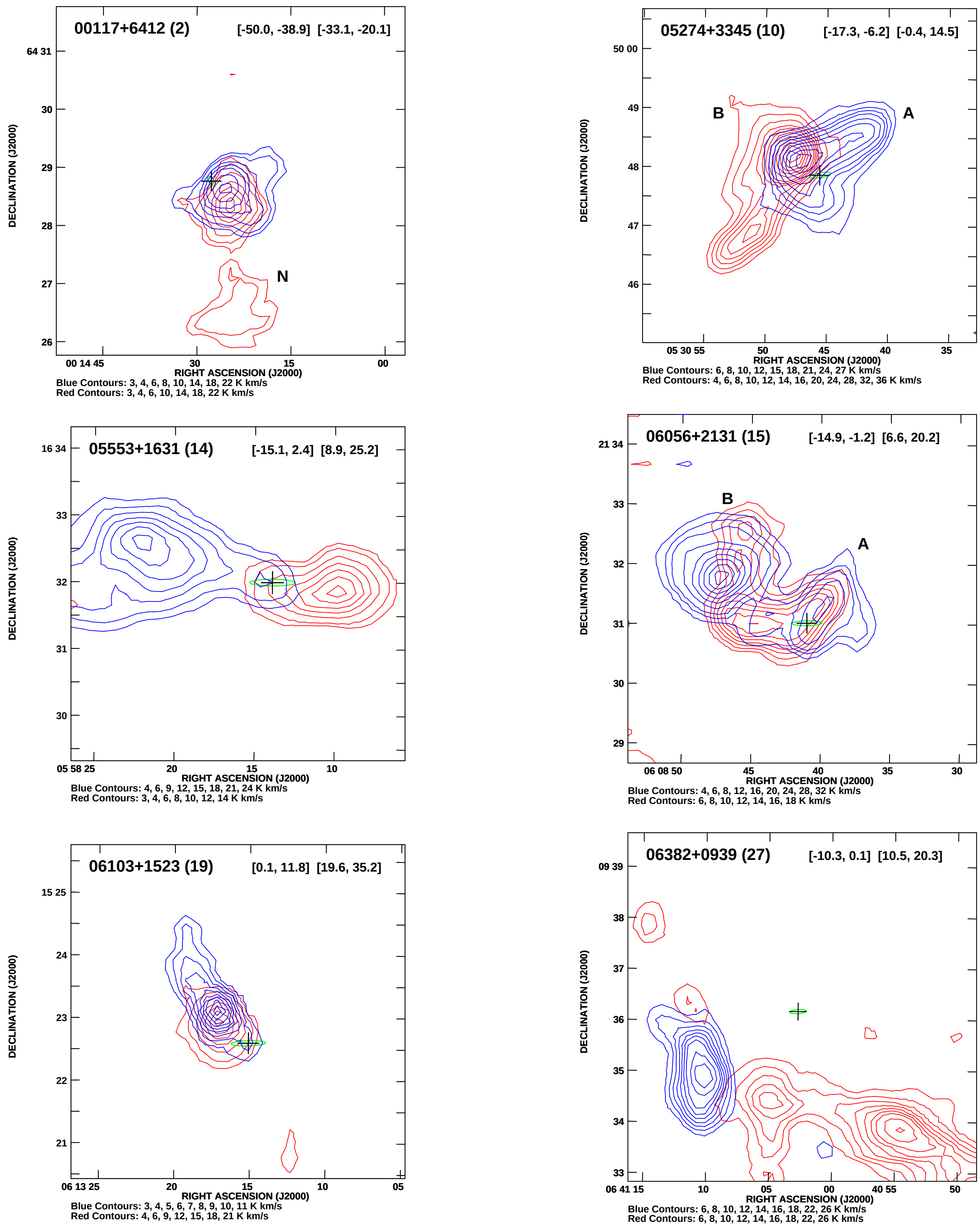

Fig. 1.— CO J=2−1 line integrated intensity maps. The Molinari source designation is given in parentheses following the IRAS name. Blue contours represent blue-shifted high-velocity gas, while red contours indicate red-shifted gas. The integrated velocity ranges are presented at the top right corner of each panel. Contour levels are listed at the bottom in each panel. The cross and its associated ellipse show the position of the IRAS point source and its uncertainty, respectively. The first and last panels show features marked by "N" which were not included when deriving the outflow parameters. In the first panel (IRAS 00117+6412) the "N" contours are a separate velocity component, whereas in the last panel (IRAS 23545+6508) the contribution of the "N" component is not well-determined because it is not fully imaged.

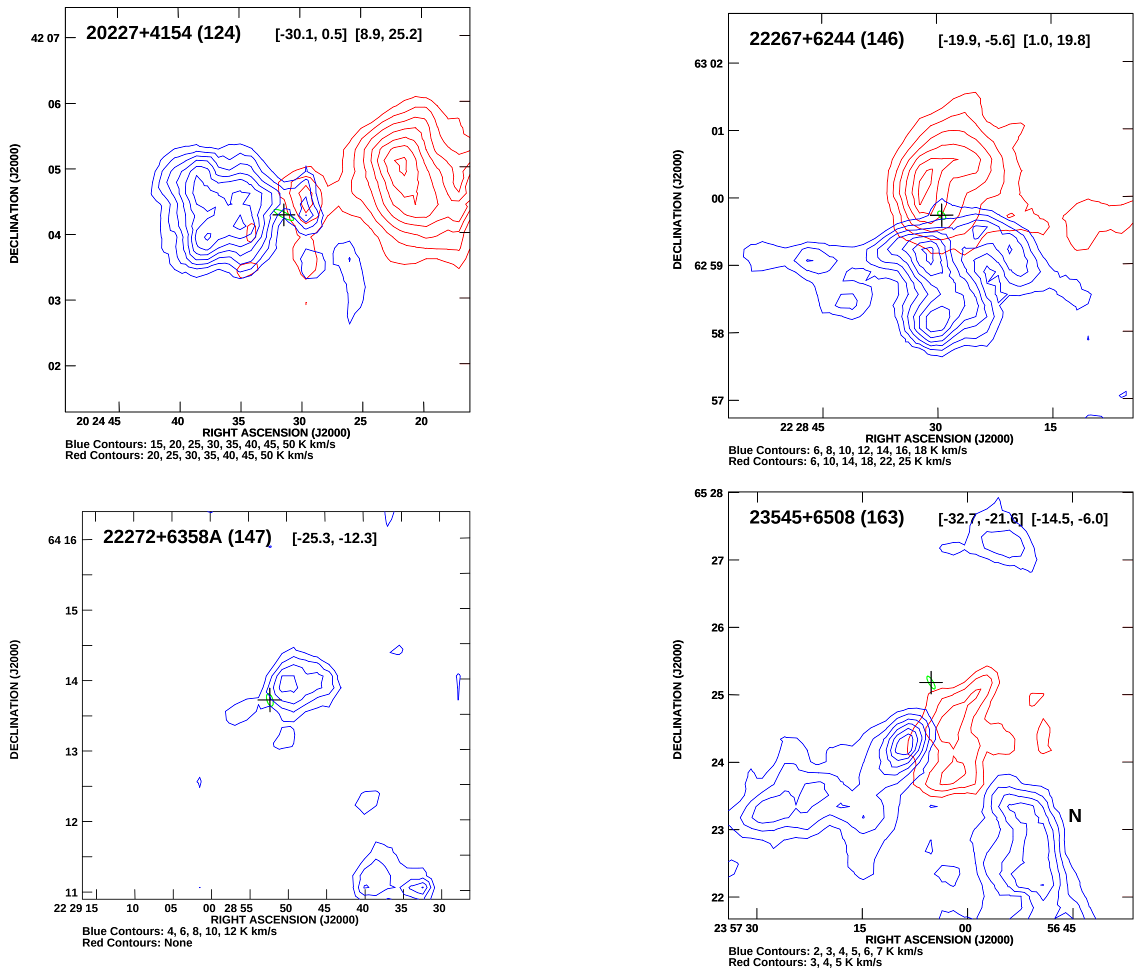

Fig. 1.— *Continued*

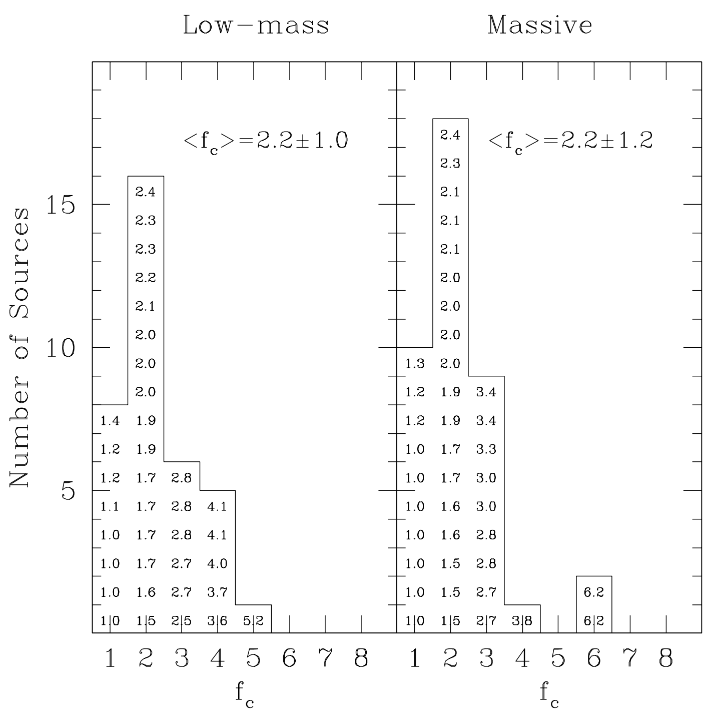

Fig. 2.— Frequency distributions of collimation factors for (*left*) 36 low-mass outflows and (*right*) 40 massive outflows. The values are listed in each bin. The two groups have the same average value, 2.2.